Aromatic Hydrocarbons and Halocarbons at a Mountaintop in Southern China

Minmin Yang[1], Yan Wang[1*], Jianmin Chen[1*], Hongli Li[2], Yuhua Li[2]

[1] *School of Environment Science and Engineering, Shandong University, Jinan, Shandong 250100, China*
[2] *Shandong Environmental Monitoring Center, Jinan, Shandong 250101, China*

ABSTRACT

In this study, 45 ambient samples were collected in the summer of 2011 and spring of 2012 on Mount Lushan. The concentrations and seasonal distributions of aromatic hydrocarbons and halocarbons were measured and discussed. Moderate concentrations of individual species were found compared with other mountain sites; however, the measured concentrations were much lower than the values reported in cities. For aromatic hydrocarbons, benzene and m/p-xylene were the most abundant species in the spring, while benzene and toluene exhibited the largest contributions in the summer. For halocarbons, the concentrations of 1,2,4-trichlorobenzene, dichlorodifluoromethane and chloromethane were higher than other gases measured in the spring; and dichlorodifluoromethane and chloromethane contributed largest in the summer. The OH loss rates demonstrated that 1,3,5-trimethylbenzene and 1,2,4-trimethylbenzene were the dominant aromatic hydrocarbons for OH loss rates in the spring, while styrene and toluene contributed the largest to reactivity in the summer. For the ozone formation potential (OFP), 1,2,4-trimethylbenzene and m/p-xylene accounted for the largest fraction of the OFPs in the spring (24.3% and 23.7%), while toluene was the most abundant source of OFP (i.e., 43.7%) in the summer. M/p-xylene exhibited large contributions to OFP in both spring and summer (23.7% and 19.2%) of the OFPs. The T/B (0.80 and 0.73 in spring and summer respectively) ratios indicated that the sampled air masses were primarily influenced by automotive emissions. The 36-h backward trajectories of the sampled air masses and the corresponding daily concentrations of individual species suggested that long-range transport had a large effect on the atmosphere at the sampling site.

Keywords: Aromatic hydrocarbons; Halocarbons; Reactivity; OFP; Backward trajectories.

INTRODUCTION

Mount Lushan is located in southern China with an altitude 1165m. The development of tourism and related industries, including restaurants and painting, has produced additional pollutants at Mount Lushan in recent decades. In recent years, the problem of air quality has become a major concern (Sun *et al.*, 2010). Aromatic hydrocarbons and halocarbons significantly contributed to the air pollution and OH loss in the atmosphere which can generate secondary pollutants and photochemical smog (Volkamer, Jimenez *et al.*, 2006). Aromatic hydrocarbons and halocarbons are two important categories of volatile organic compounds that are typically emitted from both biogenic and anthropogenic sources. However, it is challenging to define and identify a general source for these compounds because there are numerous types of compounds and abundant emitted sources in this family.

The rapid development of the economics in the East Asia region, especially in China, is associated with an inevitable increase in air pollutants. Aromatic hydrocarbons and halocarbons are emitted from various sources, mobile or stationary (Wang *et al.*, 2012), including industrial processes and solvents (Lai *et al.*, 2005; Lanz *et al.*, 2008), biogenic emissions(Guenther *et al.*, 2006; Pugh *et al.*, 2013; Wagner and Kuttler, 2014), motor vehicles, fuel storage and combustion (Lanz *et al.*, 2008), biomass burning (Wang *et al.*, 2014), and gasoline- or diesel-powered machinery (Demir *et al.*, 2012), which have received much attention in recent years. Most aromatic hydrocarbons are listed as toxic air pollutants, such as benzene, or potential toxic air contaminants, such as toluene and xylene (Hanson, 1996). Aromatic hydrocarbons, such as benzene, toluene, xylenes and trimethylbenzenes, are important components of gasoline, reformulated gasoline, vehicle emissions and ambient air in urban areas (Lonneman *et al.*, 1986; Kwok *et al.*, 1997).

Aromatic hydrocarbons are important precursors of ground-level ozone and play an important role in the formation of ozone and secondary organic aerosols (Carter, 1994; Liu *et al.*, 2008a). Once the compounds are released into the atmosphere,

---

* Corresponding author.
 Tel.: 053188361157; Fax: 053188361157
 E-mail address: wy@sdu.edu.cn; jmchen@sdu.edu.cn

most aromatic compounds are released into the air and react rapidly with OH and can participate in the formation of photochemical smog in the presence of nitrogen oxides. Hence, the abundance and speciation of aromatic hydrocarbons in the atmosphere significantly affects the ambient atmospheric chemistry (Monod *et al.*, 2001). It has also been reported that O_3 chemical production can be influenced by the concentrations of volatile organic compounds, and different species (e.g., aromatics) have different contributions to the ozone photochemical formation. Thus, identification of the emission sources of these species and their contributions to ozone formation are a crucial issue for the development of an effective O_3 control strategy (Tang *et al.*, 2007, 2008). The reaction products from the atmospheric oxidation of individual species include potential toxic and mutagenic compounds, such as aromatic aldehydes, dicarbonyls and secondary organic aerosols (Kwok *et al.*, 1997, Kleindienst *et al.*, 1999). Secondary pollutants, such as ozone that is generated in photochemical reactions are often more toxic than their precursor compounds. Therefore, it is important to accurately determine the atmospheric concentrations of the aromatic hydrocarbons. It is also important to identify primary sources and contributions of various aromatic hydrocarbons to ozone formation potential in the atmosphere. Ratio analysis was used to identify the emission sources of aromatic hydrocarbons and halocarbons in this study. In addition, detailed speciation and quantification of the measured species in the atmosphere are also necessary. In this study, two common methods, OH loss rate and the ozone formation potential, are used to estimate the reactivity of aromatic hydrocarbons in the atmosphere.

China is one of the most important halocarbon emitters in the world (Wang *et al.*, 2014) and they are of vital concern due to their toxicity and key role in ozone layer deleption and global warming. Since 1970s, halocarbons have been comprehensively studied in different countries around the world due to their association with global environmental effect, including chlorofluorocarbons (CFCs), hydrochlorofluorocarbons (HCFCs) and other halocarbons. During the implementation of the Montreal Protocol, national and regional levels of emission inventories around the world have been established to examine and predict the influence of control policies on the environment (Handl 1997; Chang *et al.*, 2001). The measured concentrations of halocarbons are actually the result of emission sources and physical or chemical transformations, thus field measurements are important and Mount Lushan was selected in this research. Halocarbons (methyl iodide, bromoform and dibromomethane) are produced naturally and the source has been found to be largely from the ocean (Sentian *et al.*, 2015), and they can be transported into the boundary layer and troposphere where they take part in ozone depletion (Montzka *et al.*, 1996; Simpson *et al.*, 2007). CFCs were widely introduced in refrigeration (CFC-12, HCFC-22), air-conditioning, foam blowing (CFC-11, CFC-22) and industrial solvent applications especially.

While many studies focused on concentrations of halocarbons in urban area and emission sources from the sea, only a few studies have focused on concentrations of halocarbons in high mountains. Pollutants emitted into the atmosphere disperse regionally and can be transported to remote places through atmospheric transport, and the influence of long-range transport is analyzed in this study. High mountains are frequently considered as the most pristine continental areas on Earth (Arellano *et al.*, 2011). Thus, the concentrations and distributions of aromatic hydrocarbons and halocarbons measured at high mountain sites can provide valuable information regarding long-range transport, which can assist in understanding the effects on the ambient concentrations and distributions.

Recent studies regarding aromatic hydrocarbons and halocarbons have focused on average mixing ratio analysis (Barletta *et al.*, 2005; Liu *et al.*, 2012) receptor modeling, emission sources (Yurdakul *et al.*, 2013; Sindelarova *et al.*, 2014) and reactivity or the ozone formation potential (Suthawaree *et al.*, 2012) in urban areas, especially in developed regions, such as Beijing, Shanghai and the Pearl River Delta Region. Few studies regarding the concentration characteristics and distributions have been conducted in remote and high-altitude locations, such as high mountain sites. In order to understand the concentration levels, photochemical reactions and emission sources of the aromatic hydrocarbons and halocarbons at high-altitudes in northern China, the measurement of the compounds was essential. This study was performed at the meteorological observation station located on the summit of Mount Lushan in northern China, which is at an altitude of 1165 m. In addition, Mount Lushan is located between the boundary layer and troposphere (free troposphere). Thus, it is an ideal site to learn the influences of the long-range transport on levels of pollutants (aromatic hydrocarbons and halocarbons in this reseach).

MATERIAL AND METHODS

Description of Sampling Site

The sampling campaign was conducted at Mount Lushan in the spring of 2012 and the summer of 2012. Mount Lushan is located in southern China (29.58N, 115.98E; Fig. 1) and it is a famous scenic area that attracts numerous tourists every year, which may increase pollutant concentrations in the surrounding area. As shown in Fig. 1, the sampling site faces the East China Sea and Yellow Sea to the east and may be influenced by air masses originating from them, especially due to long-range transport from developed coastal cities which may bring pollutants from industrial processes or marine natural products, such as chloromethane or bromoethane to the site. In recent decades, the rapid development of tourism has promoted the growth of related infrastructure, which has increased the pollutant concentrations. Most of the residents who have settled in the town of Guling, which is a local town that is located near the study site at the top of Mount Lushan, work in tourism or related services, which also enhance local pollution. Therefore, the air masses that were sampled at the Mount Lushan may contain a mixture of pollutants due to the both local sources and the long-range transport of pollutants.

The sampled air masses originated primarily from the
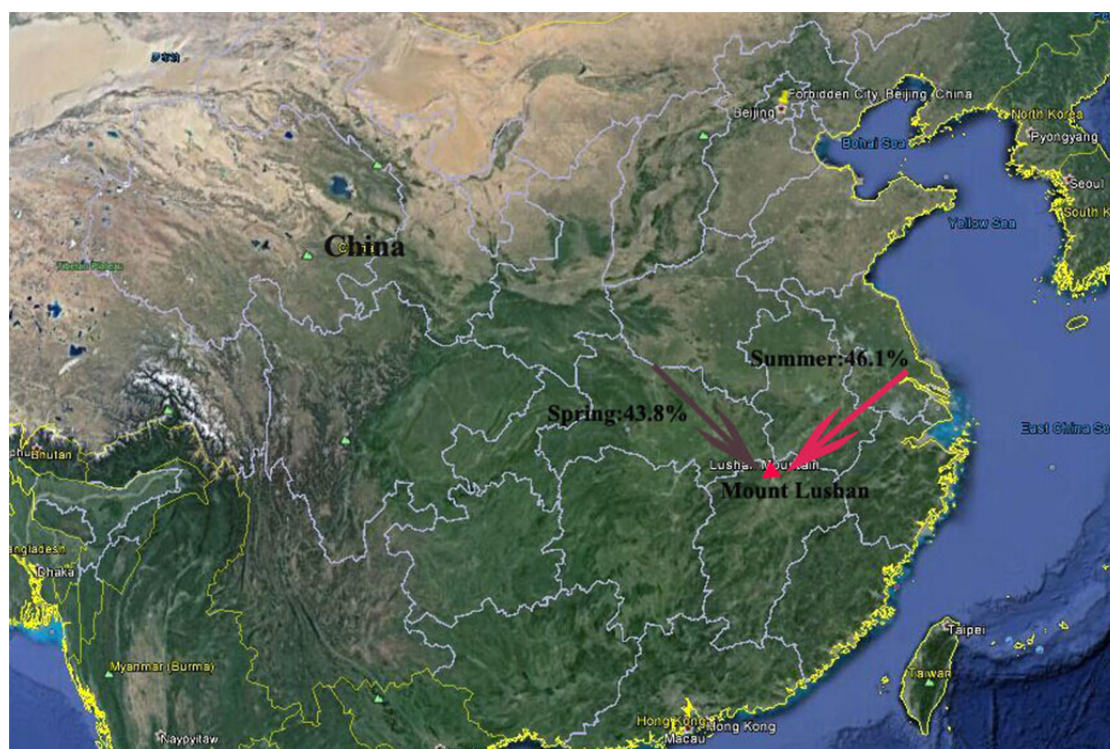
Fig. 1. The geographical position of Mount Lushan and the dominant air mass transport directions in the spring and summer.

northwest direction in the spring, while the northeast direction was dominant during sample collection in the summer based on the Hybrid Single-Particle Lagrangian Integrated Trajectory (HYSPLIT) model. Most industries such as the Lushan Small and Middle Innovation Service Center in the northwest and small and moderate-sized factories are located to the north and northwest of Mount Lushan; therefore, air masses can be transported to the site and increase the concentrations of the measured species (see Fig. S1(a)). In addition, traffic exhaust is an important source of the measured pollutants, especially aromatic hydrocarbons, which may be influenced by air masses originating from the south or southwest of the study site, which corresponds to a region with numerous highways (see Fig. 1(b)).

Sampling

The sampling campaign was conducted in the summer of 2011 (from August 17 to September 23) and the spring of 2012 (from March 21 to May 18) at Mount Lushan. Sampling and analysis were based on the USEPA methods TO-14 and TO-15. The ambient air samples were collected in fused silica-lined stainless steel vacuum canisters (SUMMA); the canisters were 3.2 L and 6 L in volume. Before collecting samples, the canisters were evacuated to < 100 mtorr and pressurized to 20 psi with humid nitrogen in three cycles using a Canister Cleaner 3100. Most of the targeted compounds had good recoveries of more than 87% over 30 days. Samples were collected during periods of 3 h to 9 h. The flow rate was controlled by a valve and the sampling was conducted every day from 9:00 to 16:00 except on very rainy and/or foggy days. The canisters were ultimately

analyzed in the laboratory within 30 days.

Analysis

Aromatic hydrocarbons and halocarbons were pre-concentrated using an Entech7100 pre-concentrator and analyzed using a GC–MS system (GC/MS QP 2010). A total of 39 species were detected in this research. For the GC–MS system, 500 ml of air with a flow rate of 100 mL min^{-1} was concentrated when passing through the instrument. The air samples were mixed with internal standards and pumped into the pre-concentrator using a three-stage cryotrap (Module 1–3). First, the air samples were concentrated using a glass bead trap (module 1), which was maintained at –150°C using liquid nitrogen. Then, the samples were recovered by desorbing at 10°C to leave most of the liquid water behind in the first trap. The trapped analytes were subsequently baked at 150°C for 5 min and transferred to module 2. The second cryotrap was maintained at –30°C, which permitted the trapped compounds to pass through to leave the carbon dioxide behind. The concentrated components were again desorbed at 180°C for 2.5 min and subsequently concentrated at the cold top of the capillary column in Module 3, which was cooled to –160°C using liquid nitrogen. Finally, the highly concentrated compounds were rapidly desorbed at 180°C and swept into the column for separation and analysis. The schematic of the preconcentration system is displayed in Fig. S2. Helium (99.999%) was used as the purge gas for the cryogenic pre-concentrator and carrier gas for the GC. The chromatographic conditions were as follows. A DB-624 column (60 m × 0.32 mm × 1.8 µm) with an injection split ratio 30: 1 was

used. The column oven temperature was held at 35°C for 5 min initially, increased to 150°C at a rate of 5°C·min⁻¹, and finally raised to 220°C at a rate of 15°C·min⁻¹ for 20 min. The column flow was 1.6 mL min⁻¹. The ionization source temperature and interface temperature was 200°C and 250°C, respectively.

The internal standards were bromochloromethane (used to quantify dichlorodifluoromethane, dichlorotetrafluoroethane, chloromethane, chloroethylene, bromomethane, chloroethane, dichloromethane, trichlorofluoromethane, 1,1-dichloroethene, trichlorotrifluoroethane, 1,1-dichloroethane, cis-1,2-dichloroethene, chloroform and 1,1,1-trichloroethane), 1,4-difluorobenzene (used to quantify tetrachloromethane, benzene, 1,2-dichloroethane, trichloroethylene, 1,2-dichloropropane, cis-1,3-dichloro-1-propene, toluene), chlorobenzene-d5 (used to quantify trans-1,3-dichloro-1-Propene, 1,1,2-trichloroethane, chlorobenzene, tetrachloroethylene, 1,2-dibromoethane, ethylbenzene, m/p-xylene) and 3-bromofluorobenzene (used to quantify o-xylene, styrene, 1,1,2,2-tetrachloroethane, 1,3,5-trimethylbenzene, 1,2,4-trimethylbenzene, 1,3-dichlorobenzene, 1,4-dichlorobenzene, 1,2-dichlorobenzene, 1,2,4-trichlorobenzene, hexachloro-1,3-butadiene). Internal standard gases were added to each sample before analysis to trace the analytical procedure. The final concentrations of the internal standards in the canisters were 2.04 ppb, 2.06 ppb, 2.08 ppb and 2.04 ppb, respectively.

Each target species was identified according to its retention time and m/z based on USEPA standard gases and the analysis was conducted under the SIM mode. The target compounds were quantified using the internal standard method with multi-point standard curves; the four compounds (bromochloromethane, 1,4-difluorobenzene, chlorobenzene-d5 and 3-bromofluorobenzene) were used as internal standards for calibrating the analytical system. The correlation coefficients of the curves, which ranged from 0.900 to 1.000, demonstrated that the integrated areas of peaks were proportional to the concentrations of the target compounds.

HYSPLIT Model

The HYSPLIT (Hybrid Single-Particle Lagrangian Integrated Trajectory) is a useful air trajectory model for studying the long-range transport of air masses (Mao *et al.*, 2009; Cheng *et al.*, 2010; Zhang *et al.*, 2014). The model is used for computing simple air parcel trajectories and complex dispersion and deposition simulations. The intial development was a result of a joint effort between NOAA and Australia's Bureau of Meteorology (http://www.arl.noaa.gov/HYSPLIT_info.php). The model is designed for quick response to atmospheric emergencies, diagnostic case studies, or climatological analyses using previously gridded meteorological data (Draxler and Hess, 1998).

Back-trajectory analysis is useful for determining the probable routes of pollutant transport to a receptor site, especially for a high-elevation site, and has been widely adopted in investigations of the influence of atmospheric transport on pollutants. 72-h backward trajectories were computed to elucidate possible routes of pollutant transport and the back trajectories were recorded every 6 h. The air masses were categorized into four categories based on the primary direction of movement near the study site, namely northeast (NE), northwest (NW), southwest (SW) and southeast (SE).

RESULTS AND DISCUSSION

General Characteristics of Aromatic Hydrocarbons and Halocarbons

Characteristics of Aromatic Hydrocarbons

A total of 13 samples was collected in the summer of 2011 (from August 17 to September 23), while 32 samples were collected in the spring of 2012 (from March 21 to May 18). Nine species of aromatic hydrocarbons and thirty halocarbons were measured in the samples collected on Mount Lushan during the monitoring period. The distributions of individual aromatic hydrocarbon concentrations are listed in Table 1 and the contributions of individual compounds to the total are displayed in Fig. 2. For the sampled aromatic hydrocarbons, benzene and m/p-xylene were the most abundant compounds in spring, with average concentrations of 0.42 ppb and 0.39 ppb, accounting for 18.3% and 17% of the total concentrations, respectively, while the dominant compounds were benzene and toluene in summer, with average concentrations of 1.15 ppb and 0.87 ppb, accounting for 46.1% and 34.7%, respectively. Specifically, benzene and toluene contributed more than 80% of the total in summer while these two compounds contributed only 33.8% in the spring. Furthermore 1,3,5-TMB and 1,2,4-TMB contributed the least in the summer with only 0.6% and 1.3% respectively. The increase in photochemical reactions in summer caused by the presence of stronger sunlight led to lower concentrations of 1,3,5-TMB and 1,2,4-TMB in summer (Lee *et al.*, 2002, Filella and Penuelas, 2006). Besides, most of the air samples collected in spring were from the northwest where many factories were located as shown in Fig. 1 which explained higher concentrations of individual aromatics except benzene and toluene in spring. The total concentrations of aromatic hydrocarbons was 2.32 ppb in spring, nearly equivalent to the concentrations measured in the summer (i.e., 2.64 ppb).

Due to the small number of samples collected in the summer of 2011, only samples collected in the spring were used for comparisons in this study. For aromatics, comparisons of individual species with other sampling sites are shown in Table S1. The total aromatic concentration measured on Mount Lushan was 2.32 ppb. This value is slightly higher than the result reported on Mount Tai (1.58 ppb) (Mao *et al.*, 2009), which is located to the east of the North China Plain, and lower than that reported for Gongga Mountain (2.75 ppb) in southeastern Sichuan Province (Zhang *et al.*, 2014) and Dinghu Mountain (5.75 ppb) in Guangdong Province (Tang *et al.*, 2007). The concentrations measured on Mount Lushan are much higher than those reported on Mount Wuyi (0.47 ppb) and in the Greater Higgnan Mountains (0.59 ppb) set as background sites. Moreover, the concentrations measured on Mount Lushan are much lower than those from urban areas, such as Beijing (11.03 ppb) (Wu *et al.*, 2010). The average concentration of 1,3,5-TMB was 0.24 ppb at Mount Lushan, close to that

Table 1. The concentration distributions of aromatic hydrocarbons and halocarbons (ppb).

Compound	MDL	Spring		Summer	
		Range	Average	Range	Average
Aromatic Hydrocarbons					
Benzene	0.110	0.16–0.84	0.42	0.41–1.74	1.15
Toluene	0.015	0.08–1.3	0.36	0.27–2.64	0.87
Ethylbenzene	0.005	nd[a]–0.92	0.19	nd[a]–0.24	0.13
m/p-Xylene	0.005	0.08–1.61	0.39	0.06–0.27	0.17
o-Xylene	0.005	nd[a]–0.12	0.17	nd[a]–0.07	0.04
Styrene	0.005	nd[a]–1.98	0.18	nd[a]–0.25	0.09
1,3,5- TMB[b]	0.005	nd[a]–3.55	0.24	nd[a]–0.03	0.16
1,2,4- TMB[c]	0.011	0.08–5.88	0.36	nd[a]–0.10	0.03
Halocarbons					
Dichlorodifluoromethane	0.144	0.35–0.70	0.54	0.40–1.29	0.74
Dichlorotetrafluoroethane	0.055	nd[a]–0.14	0.07	nd[a]–0.08	0.04
Trichlorofluoromethane	0.050	0.11–0.38	0.26	0.22–0.50	0.34
Trichlorotrifluoroethane	0.050	0.05–0.21	0.13	0.08–0.19	0.13
Chloromethane	0.062	nd[a]–1.28	0.51	nd[a]–3.46	1.71
Chloroethylene	0.029	nd[a]–0.13	0.06	nd[a]–0.06	0.02
Bromomethane	0.036	nd[a]–0.14	0.07	nd[a]–0.05	0.03
Chloroethane	0.014	nd[a]–0.17	0.08	nd[a]–0.08	0.05
1,1-dichloroethene	0.033	nd[a]–0.12	0.06	nd[a]–0.06	0.01
Dichloromethane	0.033	0.11–0.78	0.38	0.14–1.05	0.48
1,1-dichloroethane	0.033	nd[a]–0.13	0.06	nd[a]–0.07	0.02
Cis-1,2-dichloroethene	0.022	nd[a]–0.16	0.07	nd[a]–0.03	0.01
Trichloromethane	0.033	nd[a]–0.70	0.23	0.14–1.80	0.48
1,1,1-trichloroethane	0.056	nd[a]–0.13	0.06	nd[a]–0.07	0.02
Tetrachloromethane	0.050	0.06–0.21	0.14	0.13–0.26	0.18
1,2-dichloroethane	0.050	0.05–0.52	0.22	0.19–1.25	0.60
Trichloroethylene	0.015	nd[a]–0.26	0.10	nd[a]–0.03	0.02
1,2-dichloropropane	0.008	nd[a]–0.26	0.14	nd[a]–0.25	0.11
Cis-1,3-dichloro-1-Propene	0.055	nd[a]–0.24	0.08	nd[a]–0.07	0.03
Trans-1,3-dichloro-1-Propene	0.017	nd[a]–0.41	0.08	nd[a]–0.09	0.03
Ethane-1,1,2-trichloro-	0.027	nd[a]–0.18	0.10	nd[a]–0.28	0.11
Tetrachloroethylene	0.050	nd[a]–0.18	0.08	nd[a]–0.06	0.03
1,2-dibromoethane	0.006	nd[a]–0.36	0.09	nd[a]–0.03	0.01
Chlorobenzene	0.004	nd[a]–0.24	0.10	nd[a]–0.08	0.04
1,1,2,2-tetrachloroethane	0.002	nd[a]–0.20	0.11	nd[a]–0.01	0.01
1,3-dichlorobenzene	0.005	nd[a]–0.29	0.15	nd[a]–0.02	0.01
1,4-dichlorobenzene	0.004	0.06–0.31	0.17	nd[a]–0.33	0.08
1,2-dichlorobenzene	0.005	0.06–0.35	0.19	nd[a]–0.04	0.03
1,2,4-trichlorobenzene	0.075	0.19–2.04	1.20	nd[a]–1.06	0.61
Hexachloro-1,3-butadiene	0.071	nd[a]–0.42	0.17	nd[a]–0.42	0.21

[a] not detected.

[b] 1,3,5-trimethylbenzene.

[c] 1,2,4-trimethylbenzene.

in Beijing with 0.29 ppb; 1,2,4-TMB concentration was 0.36 ppb, lower than that in Beijing with 0.72 ppb, while close to that in Gongga Mountain (0.39 ppb). Concentrations of BTEX were higher than the background sites Mount Wuyi (0.47 ppb) and in the Greater Higgnan Mountains (Lyu *et al.*, 2013) was measured at moderate levels compared with other high mountain sites.

Characteristics of Halocarbons

The concentration distributions of halocarbons are listed in Table 1. The most abundant halocarbons were 1,2,4-trichlorobenzene, dichlorodifluoromethane and chloromethane in the spring, with average concentrations of 1.20 ppb, 0.54 ppb and 0.51 ppb, respectively, while the dominant compounds were chloromethane and dichlorodifluoromethane in the summer, with average concentrations of 1.71 ppb and 0.74 ppb, respectively. The concentrations of individual halocarbons varied from 0.06 ppb to 1.20 ppb in the spring and from 0.01 ppb to 1.71 ppb in the summer. Four common chlorofluorocarbons (CFC) were measured in this study, including trichlorofluoromethane (CFC-11), dichlorodifluoromethane
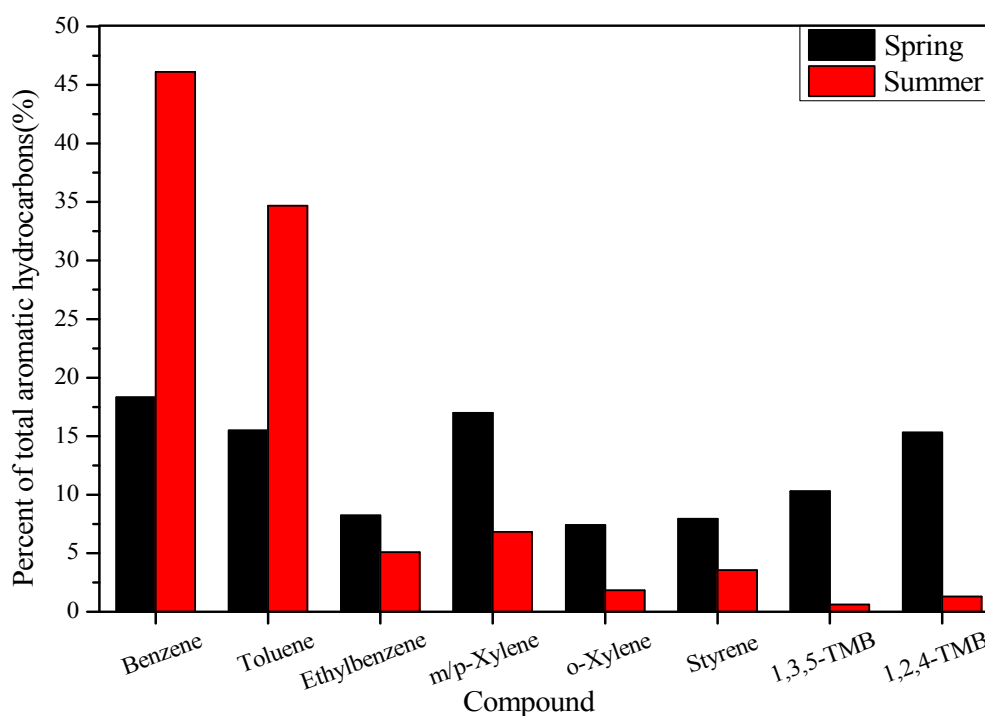
Fig. 2. The percent contribution of the individual aromatic hydrocarbons to the total concentrations in the spring and summer.

(CFC-12), trichlorotrifluoroethane (CFC-113) and dichlorotetrafluoroethane (CFC-114); comparisons of selected halocarbons with measurements from other mountain sites are listed in Table 2. The comparison is limited to only a few halocarbons due to the lack of data for other mountain sites. CFCs were widely used in refrigeration, air-conditioning, foam blowing and industrial solvent applications (Kim *et al.*, 2011). The chemical stability and high volatility of CFCs allow these compounds to remain in the atmosphere for a long time once released and to gradually diffuse into the stratosphere (Molina and Rowland, 1974, Kim *et al.* 2011). The long lifetimes of the four halocarbons measured in this study were estimated using various methods; typical estimates for their lifetimes are 43–186 years (Martinerie *et al.*, 2009). Hence, the concentration distributions of long-lived CFCs are influenced by the interactions among emission sources, long-range transport and chemical losses into the atmosphere. The CFC concentration distributions were approximately equal in spring and summer due to their long lifetimes and thorough atmospheric mixing as well as the four species being emitted from anthropogenic sources (Seinfeld and Pandis, 2006). As shown in Table 2, the CFC concentrations measured in this study are generally higher than those reported for background sites on Mount Wuyi and in the Greater Higgnan Mountains (Lyu *et al.*, 2013). According to Montreal Protocol, a small quantity of CFCs is still used in China, and Mount Lushan is located in the free troposphere where long life-time CFCs existed (Tang *et al.*, 2006), which accounted for higher concentrations of CFCs than the background sites. The concentration of CFC-113 was 0.13 ppb, which is higher than that measured on Mount Tai (Mao *et al.*, 2009) and Gongga Mountain

(0.09 ppb) (Zhang *et al.*, 2014), while the concentration of CFC-11 measured herein was nearly equal to that at the other mountain sites. However, the concentration of CFC-114 was substantially higher than that measured at Gongga Mountain (0.02 ppb).

Concentration of trichloromethane (0.23 ppb) was higher at Mount Lushan than that reported at Mount Tai (0.05 ppb) (Mao *et al.*, 2009) and Gongga Mountain (0.20 ppb) (Zhang *et al.*, 2014), but lower than Mount Wuyi (0.34 ppb) and Greater Higgnan Mountains (0.39 ppb) (Lyu *et al.*, 2013). The dichloromethane concentration was 0.38 ppb, which is similar to that measured on Mount Tai (0.30 ppb) and in the Greater Higgnan Mountains (0.31 ppb). Dichloromethane is produced during biomass burning and from anthropogenic combustion, and solvent evaporation during cleaning processes (Mao *et al.*, 2008). The chloromethane concentration was 0.51 ppb, which is much higher than that measured in the Greater Higgnan Mountains (0.01 ppb) and on Mount Wuyi (0.22 ppb) (Lyu *et al.*, 2013). However, this concentration is lower than the value reported from Gongga Mountain with 0.62 ppb (Zhang *et al.*, 2014). The main reason for this may attributed to Mount Lushan being located nearer to the sea than the other sites. The primary natural sources of chloromethane and bromomethane are oceanic processes (Tang *et al.*, 2006); the daily concentration variations of chloromethane and bromomethane are displayed in Fig. S3. The concentration of these two compounds showed similar temporal variation, indicating that most of the chloromethane and bromomethane sampled at the mountain site were emitted from the same source, most likely ocean emissions transported to the site through atmospheric advection. TCE was primarily used as solvents and degreasing in a wide

Table 2. Concentration comparison of selected halocarbons with other studies (ppb).

Compound	Mount Lushan	Mount Tai[a]	Gongga Mountain[b]	Mount Wuyi[d]	Greater Higgnan Mountains[d]
CFC-12	0.54	—	—	0.18	0.01
CFC-114	0.07	—	0.02	0.00	0.01
CFC-11	0.26	0.26	0.28	0.09	0.02
CFC-113	0.13	0.07	0.09	0.01	0.00
Chloromethane	0.51	—	0.62	0.22	0.01
Dichloromethane	0.38	0.30	0.36	0.62	0.31
Trichloromethane	0.23	0.05	0.20	0.34	0.39
1,1,1-trichloroethane	0.06	0.01	—	0.00	0.00
1,2-dichloroethane	0.22	0.60	0.25	0.26	0.06
Tetrachloroethylene	0.08	0.03	—	0.00	0.01
Chlorobenzene	0.10	0.15	0.08	0.00	0.00

[a] Mao *et al.*, 2009.
[b] Zhang *et al.*, 2014.
[d] Lyu *et al.*, 2013.

variety of industrial manufacturing and chemical processes (Lee *et al.*, 2014). As indicated above, the Lushan Small and Middle Innovation Service Center in the northwest, which includes many small and moderate-sized factories, such as glass fiber plants, auto part manufacturers, pharmaceutical factories and other industries which may all release TCE and influence Mount Lushan. The other selected halocarbon concentrations exhibited moderate concentrations compared with other mountain sites.

Measures of Aromatic Hydrocarbon Contributions to Potential Ozone Formation

The OH loss rate (L_{OH}) and the ozone formation potential (OFP) were calculated in this study to quantify contributions of the measured aromatic hydrocarbons to potential ozone production. As the majority of the halocarbons are long-lived, they are not considered for their contributions to ozone OH loss rates and OFP. Only OH losses of aromatic hydrocarbons are calculated herein. The OH loss rate (L_{OH}) is frequently used to estimate the initial peroxy radical (RO_2) formation rate, which is the key step in ozone formation in air pollution processes (Carter, 1994, Tang *et al.*, 2006). The approach does not account for all chemical processes; however, the method provides a simple way to assess the relative contribution of individual species to photochemical reactions (Goldan *et al.*, 2004). The contribution to OH loss rates L_{OH} can be calculated as

$$L_{OH} = c_i \cdot k_i^{OH}. \tag{1}$$

The coefficient k_i^{OH} represents the rate constant of individual species at 298 k and 1 atm, while c_i represents the ambient concentration of individual species. The values of k_i^{OH} for the individual species were published by Atkinson (Atkinson and Arey, 2003); these values have been used in many studies (Seinfeld and Pandis, 2006, Liu *et al.*, 2008b). The L_{OH} values for individual aromatics and their contributions to the overall L_{OH} are shown in Fig. 3. Not all of these species with higher concentrations had larger contributions to OH loss. In the spring, the total contribution

of benzene, toluene and ethylbenzene to OH loss was only 4.9%, while they represented 42.0% of the total ambient concentration. 1,3,5-TMB, 1,2,4-TMB and styrene provided the largest contribution to OH loss, accounting for more than 72.0% of the overall L_{OH}, while their concentrations contributed only 33.6% of the total. The three xylene isomers contributed approximately 19.6% to OH loss, which was comparable with their total contribution to the total concentration. Therefore the largest contributors to the reactivity of aromatics were 1,3,5-TMB, 1,2,4-TMB and styrene, indicating that they were important precursors of ozone at Mount Lushan in the spring. However, the results are drastically different for the summer measurements. Styrene provided the largest contribution to OH loss, accounting for 28.5%, while it accounted for only 3.6% of the total ambient concentration. The contributions of toluene and ethylbenzene to the total concentration were 34.7% and 5.1%, respectively, which were comparable with the fractions (27.0% and 4.9%) of the overall L_{OH}. 1,3,5-TMB and 1,2,4-TMB accounted for small fractions of L_{OH}, which were very different from the percentages found in the spring. In contrast, benzene provided the most contribution (46.1%) to the total concentration; however, it only contributes a small fraction (7.8%) of the overall L_{OH}. Benzene and toluene contributed largest to the photochemical reactivity of the aromatics in the summer at Mount Lushan.

Therefore, together with 1,3,5-TMB, 1,2,4-TMB and styrene played a predominant role in the photochemical reactions in spring. Xylenes played a smaller roll in OH loss due to their low concentrations, while benzene, toluene and ethylbenzene contributed the least (4.8%) to the total OH loss. In the summer, toluene and styrene exhibited a large contribution to OH loss (55.5%) and o-xylene played only a minor role (1.8%) in the total OH loss. The results demonstrate that OH loss was more pronounced in the spring than that in the summer due to the higher aromatic concentrations. Different aromatics contributed to ozone formation or photochemical reactivity differently. Styrene was the largest contributor to OH loss at Mount Lushan in spring and summer.

The OFP is frequently used to assess the roles of species
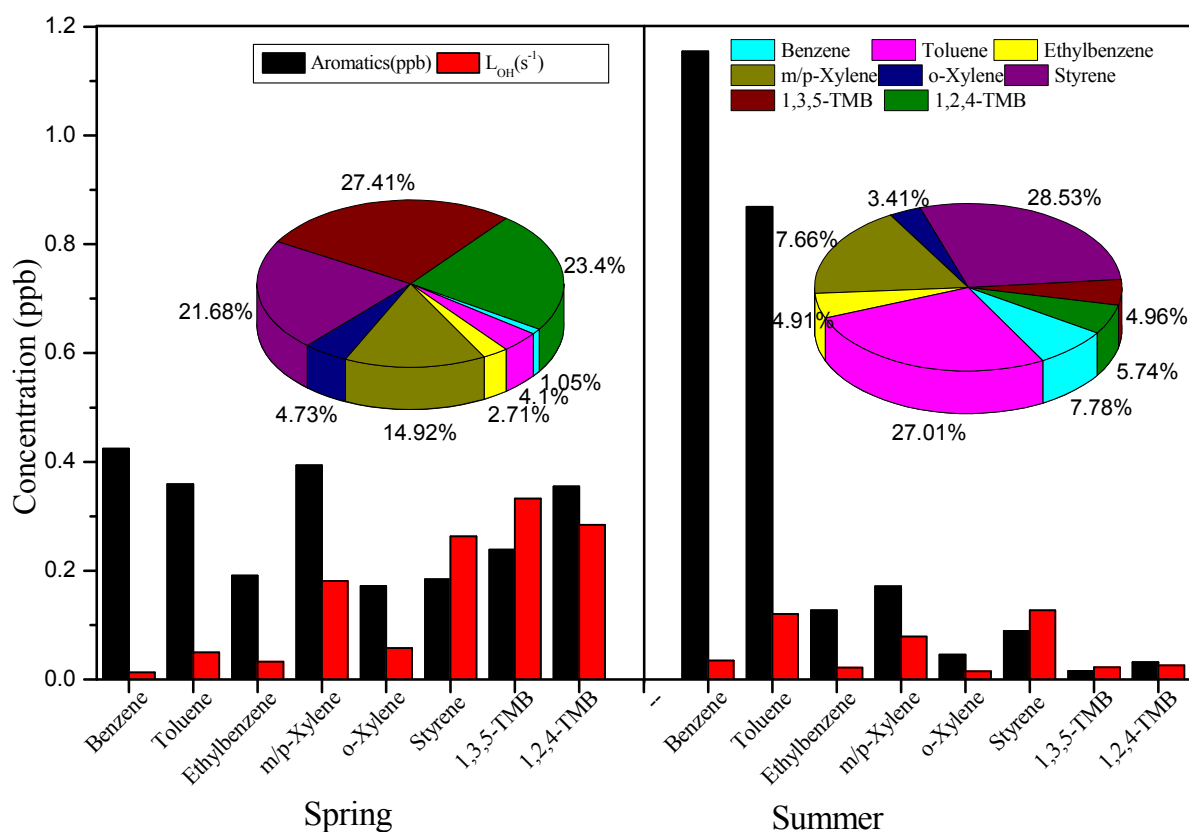
Fig. 3. The OH loss rates of aromatic hydrocarbons with their contributions in spring and summer. The pie graphs indicate the percent of total L_{OH} attributed to individual aromatic hydrocarbons.

in the process of ozone formation and to estimate the contribution to photochemical ozone formation (Carter 1994; Zheng *et al.*, 2009). The OFP of an individual species can be calculated as follows:

$$OFP = c_i \cdot MIR_i. \quad (2)$$

The constant MIR_i is the maximum incremental reactivity for each individual species i, which was obtained from (Carter 2009). The total OFP is the sum of the OFP of all individual species measured in this study. The OFP of each individual species and their contributions to the total OFP are depicted in Fig. 4. Again, not all of the species with higher concentrations had higher OFPs and exhibited larger contributions to the total OFP. In spring, 1,3,5-TMB and 1,2,4-TMB contributed more to the total OFPs, i.e., 21.6% and 24.3%, respectively, even though these compounds only accounted for 10.3% and 15.3% of the total concentration. Benzene was the most abundant species, accounting for 18.3% of the total concentration; however, it only contributed 2.32% to the total OFP. M/p-xylene was the next most abundant species, exhibiting a comparable percentage of 23.7% to the total OFPs. Toluene, ethylbenzene, o-xylene and styrene exhibited smaller contributions to the total OFP due to their low concentrations. However, due to having the lowest concentrations, styrene, 1,3,5-TMB and 1,2,4-TMB accounted for only 2.17%, 2.67% and 4.08% of the total OFPs in the summer, which were the smallest contributions

to the total OFPs. Benzene contributed the most to the total concentration while only accounting for 11.7% of the total OFPs. Toluene had the largest contribution to the total OFPs (49.7%), although its contribution to the total concentration was second. M/p-xylene represented 10.9% of the total concentration; however, it accounted for 19.2% of the total OFP. In terms of OFPs, 1,3,5-TMB, 1,2,4-TMB and m/p-xylene were the key aromatic species in the spring. Toluene and m/p-xylene were the dominant species of the total ozone formation potential in the summer.

Thus, 1,3,5-TMB and 1,2,4-TMB contributed largest to OFP in the spring, which is the same as the OH loss, indicating that the two compounds needs to be controlled in the spring to reduce the ozone pollution. Toluene played an important role in OH loss and OFP in the summer indicating that toluene is the major pollutant for control in the summer at Mount Lushan. The difference between the OH loss rate and OFP of styrene demonstrated that the L_{OH} does not account for all processes in ozone formation that are included in the calculation of the MIR used to determine OFP. Instead, OH loss provided a measure of the relative contribution of each compound to photochemical reactivity in the daytime (Tang *et al.*, 2006).

Source Identification and Influence of Long-Range Transportation on Measured Species

In the summer, the NE direction was dominant, accounting for 46.1% of the total samples; none of the collected samples
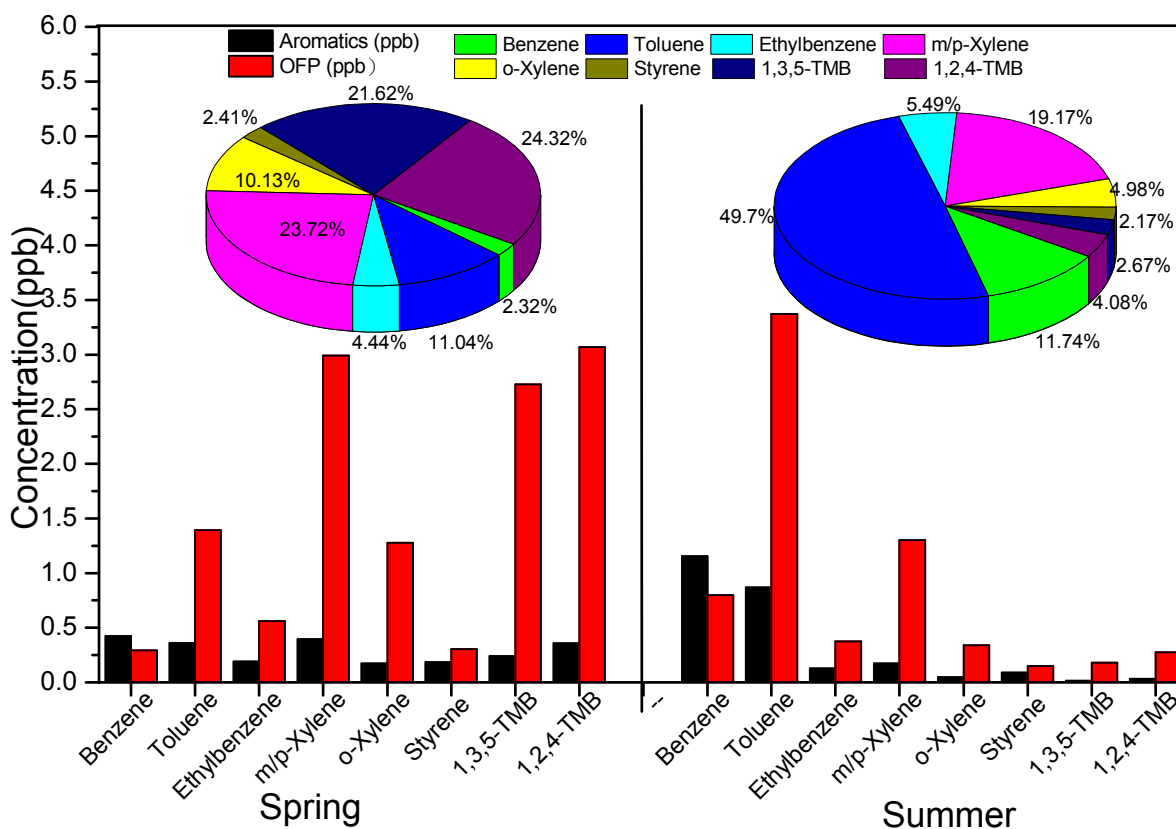
Fig. 4. The OFP of aromatic hydrocarbons and their contributions in spring and summer. The pie graphs indicate the percent of total OFP attributed to individual aromatic hydrocarbons.

originated from the NW. The SW and SE directions accounted for 23.1% and 30.8% of the total samples, respectively. In spring, the NW was dominant, accounting for 43.75% of the total samples; the SE direction contributed the least, accounting for only 12.5%. The other two directions, i.e., SW and NE, accounted for 25.0% and 18.75% of the total, respectively. As indicated above, the main emission sources may be the traffic sources and solvent use and this will be discussed later.

Because different compounds have different photochemical reactivity and emission sources, some of their ratios are frequently used to obtain primary information regarding their sources and transport (Yurdakul *et al.*, 2013). Studies of vehicular exhaust suggest that the T/B ratio can be widely used to differentiate between vehicular emissions and other combustion sources (Elbir *et al.*, 2007). Low T/B ratios (< 2.0) have been shown to be indicators of pronounced motor vehicle emissions (Oguz *et al.*, 2003; Elbir *et al.*, 2007). In this study, the average T/B ratios were 0.80 (ranging from 0.45 to 1.54) and 0.73 (ranging from 0.43–1.86) in the spring and summer, respectively, indicating the strong influence of motor vehicle emissions. Therefore, the main source of pollutants on Mount Lushan may be motor vehicle emissions.

The daily variations in the concentrations of the selected species and TVOC (the sum of the aromatic hydrocarbons and halocarbons) are shown in Fig. 5. In spring, the m/p-xylene, ethylbenzene, 1,3,5-TMB, 1,2,4-TMB, and TVOC concentrations were much higher on March 25, while the

concentrations of benzene, toluene and m/p-xylene increased on April 6 and May 8; the toluene concentrations were notably higher. Previous studies have shown that BTEX are important components of vehicular exhaust; benzene is especially related to gasoline-related emissions (Watson *et al.*, 2001; Choi and Ehrman, 2004; Zhang *et al.*, 2014). The 36-h backward trajectories calculated for these three days are shown in Fig. S5. The backward trajectories demonstrate that the air masses all originated from the northwest neighboring provinces, containing emission from Henan and Hubei Provinces. 1,3,5-TMB and 1,2,4-TMB are typical tracers used as solvents (Borbon *et al.*, 2002; Guo *et al.*, 2004). As indicated above, the Lushan Small and Middle Innovation Service Center in the northwest, may contribute to the high levels of the selected species. Tomb-sweeping day (or qingming, April 4–6) and Labor Day (May 1–3), which typically attract many visitors to the scenic area and increase vehicle exhaust emissions, may have also contributed to the higher levels.

In the summer, the concentrations of benzene and toluene were generally higher than those detected in spring, especially on September 21, when the toluene concentration exceeded the benzene concentration. The 36-h backward trajectories for summer are shown in Fig. 6. None of the sampled air masses originated from the NW. Four air masses were associated with the NE (black lines), three air masses originated from the SE (red lines), two trajectories originated from the SW (green lines) and two air masses were from local
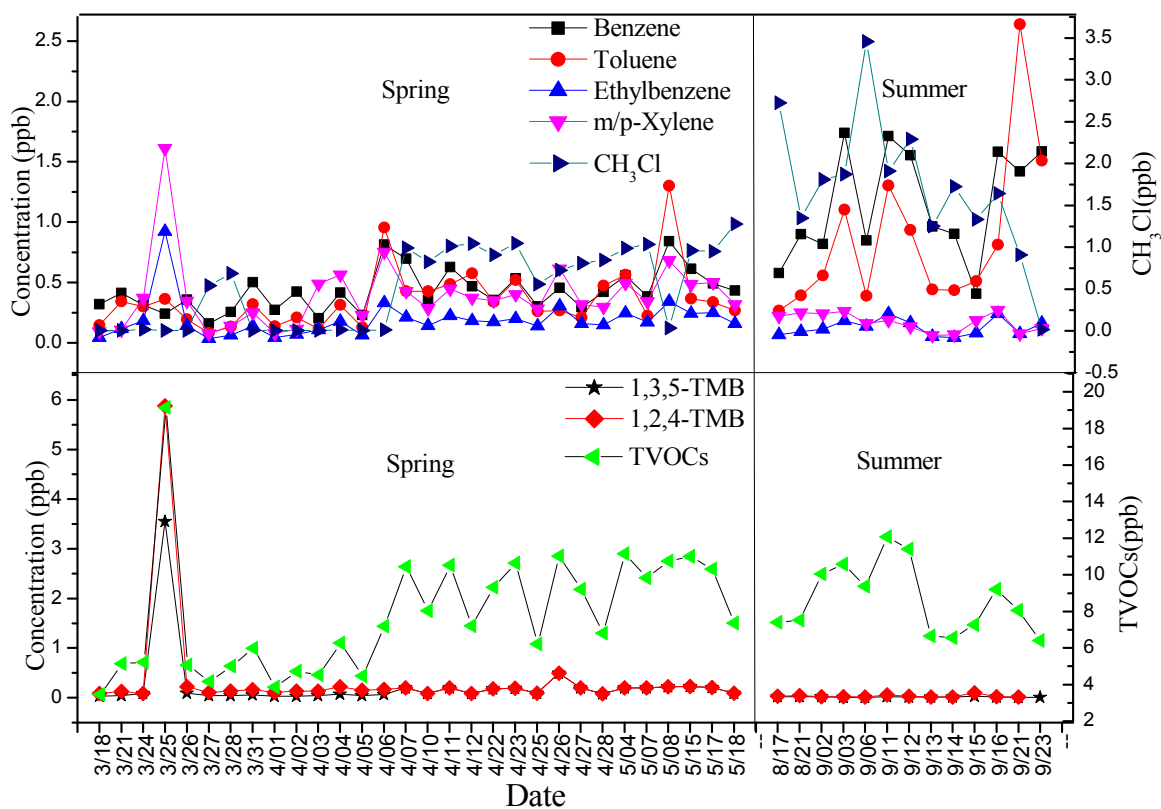
Fig. 5. Time series of concentration of TVOC and selected species (BTEX, 1,3,5-TMB, 1,2,4-TMB and CH₃Cl) in spring and summer.
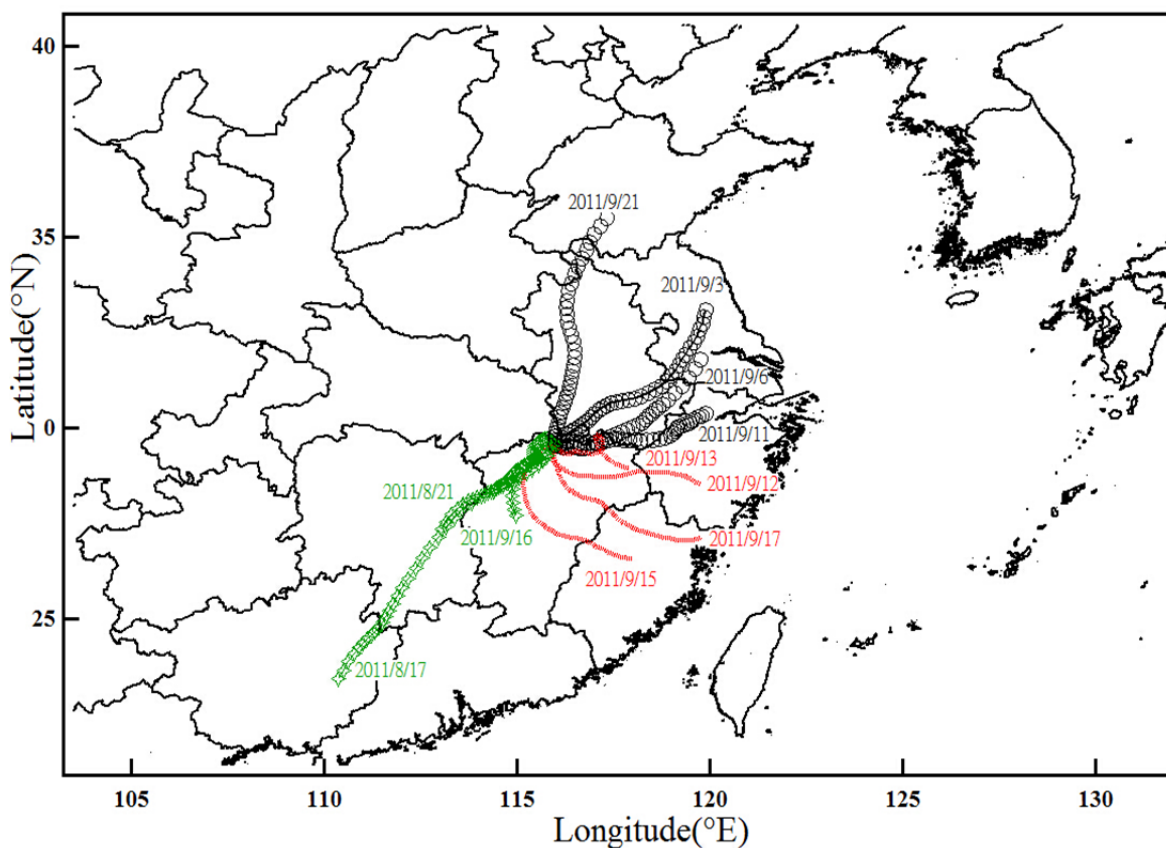
Fig. 6. The 36 h-backward trajectories of the 11 air masses sampled in the summer of 2011 at Mount Lushan.

sources (on September 13 and 16), originating from the SE and SW, respectively. Only one air mass originated from southern Shandong Province and was subsequently advected through Anhui Province, which are two developed provinces in the vicinity of the study site. The pollutants were transported to the site and resulted in higher toluene concentrations due to the emissions from industrial sources other than gasoline exhaust. The concentrations of the selected compounds were comparable on September 3 and 11; the air masses originated from the same direction, indicating that the concentrations were primarily influenced by long-range transport from northeast on these days. The concentrations of the selected compounds and TVOCs were all comparable on September 11 and 12 because the backward trajectories for these days exhibited similar trends even though they originated from slightly different directions (Fig. 6). This result also suggests that long-range transport had a large effect on the observed species concentrations. The air masses on August 17 and 21 were also indicative of long-range transport having a large effect. TVOC and the selected species were generally lower on August 17 because of dilution, which resulted from the air masses being transported through more locations. Specifically, in the summer, benzene and toluene exhibited generally higher concentrations, while the other species exhibited lower concentrations, indicating that the primary sources on Mount Lushan were from traffic and solvent use, which are both related to the rapid development of tourism and its related infrastructure or industry near Mount Lushan.

Chloromethane is typically used as a tracer in biomass/coal burning (Gao *et al.*, 2005; Barletta *et al.*, 2009; Ling *et al.*, 2011). Moreover, previous studies have shown that coal combustion can also emit significant amounts of benzene into the atmosphere (Moreira Dos Santos *et al.*, 2004). Therefore, as the chloromethane concentration increases, the benzene concentration also increases indicating the primary source is biomass/coal burning. However, in this study, the concentrations of benzene and chloromethane did exhibit different variations (Fig. 5), suggesting that coal/biomass combustion were not the contributions to the measured benzene and chloromethane concentrations. The dominant natural sources of chloromethane and bromomethane are emitted from oceanic processes (Tang *et al.*, 2006). As shown in Fig. S3, the daily concentrations of chloromethane and bromomethane are displayed. The concentration variations for these two compounds were nearly consistent, indicating that most of the chloromethane and bromomethane sampled at the mountain site were probably emitted from the ocean and subsequently transported to the site through atmospheric advection.

CONCLUSIONS

Field measurements of aromatic hydrocarbons and halocarbons were performed during the summer of 2011 and the spring of 2012 on Mount Lushan in southern China, which is an important scenic mountain with an altitude of 1165 m in southern China; the measurements were performed during the summer of 2011 and the spring of 2012. Nine species of aromatic hydrocarbons and thirty halocarbons were measured using GC-MS. Chloromethane, benzene, dichlorodifluoromethane and 1,2,4-trichlorobenzene were the most abundant species during the two seasons.

The OH loss rate (L_{OH}) and the ozone formation potential (OFP) were used to assess the OH loss and contributions to ozone formation. 1,3,5-TMB, 1,2,4-TMB and styrene were the most important precursors of ozone in the spring while benzene and toluene contributed largest to the photochemical reactivity of the aromatics in the summer at Mount Lushan. The OH loss rates were much higher in the spring than in the summer except for benzene and toluene due to their higher concentrations. OFP was used to estimate the contributions to the total photochemical ozone formation. The key aromatic species were 1,3,5-TMB, 1,2,4-TMB and m/p-xylene in the spring, and toluene and m/p-xylene were the dominant species in ozone formation in the summer.

The T/B ratio was used to identify traffic with other emission sources in this study. The smaller T/B ratios (< 2.0) suggested that motor vehicular emissions may have been the primary pollution source for those compounds. The directions and paths of the 36-h backward trajectories had pronounced effects on the corresponding selected species and total concentrations, indicating that long-range transport (most of the samples except on September 13 and 16) was important in determining the distribution of species collected at the mountain site. Traffic sources and solvent evaporation (higher benzene and toluene concentrations) were the primary sources that affected the concentrations of aromatic hydrocarbons and halocarbons measured on Mount Lushan, and ocean sources (time series of $CHCl_3$ and $CHBr_3$) also contributed to the halocarbons; biomass/coal burning and local sources (on September 13 and 16) contributed a much smaller portion.

ACKNOWLEDGMENTS

SUPPLEMENTARY MATERIALS

Supplementary data associated with this article can be found in the online version at http://www.aaqr.org.

REFERRENCES

Arellano, L., Fernandez, P., Tatosova, J., Stuchlik, E. and Grimalt, J.O. (2011). Long-range Transported Atmospheric Pollutants in Snowpacks Accumulated at Different Altitudes in the Tatra Mountains (Slovakia). *Environ. Sci. Technol.* 45: 9268–9275

Atkinson, R. and Arey, J. (2003). Atmospheric Degradation of Volatile Organic Compounds. *Chem. Rev.* 103: 4605–4638.

Barletta, B., Meinardi, S., Sherwood Rowland, F., Chan,

C.Y., Wang, X., Zou, S., Yin Chan, L. and Blake, D.R. (2005). Volatile Organic Compounds in 43 Chinese Cities. *Atmos. Environ.* 39: 5979–5990.

Barletta, B., Meinardi, S., Simpson, I.J., Atlas, E.L., Beyersdorf, A.J., Baker, A.K., Blake, N.J., Yang, M., Midyett, J.R., Novak, B.J., McKeachie, R.J., Fuelberg, H.E., Sachse, G.W., Avery, M.A., Campos, T., Weinheimer, A.J., Rowland, F.S. and Blake, D.R. (2009). Characterization of Volatile Organic Compounds (VOCs) in Asian and north American Pollution Plumes during INTEX-B: Identification of Specific Chinese Air Mass Tracers. *Atmos. Chem. Phys.* 9: 5371–5388.

Borbon, A., Locoge, N., Veillerot, M., Galloo, J.C. and Guillermo, R. (2002). Characterisation of NMHCs in a French Urban Atmosphere: Overview of the Main Sources. *Sci. Total Environ.* 292: 177–191.

Carter, W.P. (1994). Development of Ozone Reactivity Scales for Volatile Organic Compounds. *Air Waste* 44: 881–899.

Carter, W.P. (2009). Updated Maximum Incremental Reactivity Scale and Hydrocarbon Bin Reactivities for Regulatory Applications. California Air Resources Board Contract, pp. 07–339.

Chang, C.C., Lo, G.G., Tsai, C.H. and Wang, J.L. (2001). Concentration Variability of Halocarbons over an Electronics Industrial Park and its Implication in Compliance with the Montreal Protocol. *Environ. Sci. Technol.* 35: 3273–3279.

Cheng, H.R., Guo, H., Saunders, S.M., Lam, S.H.M., Jiang, F., Wang, X.M., Simpson, I.J., Blake, D.R., Louie, P.K.K. and Wang, T.J. (2010). Assessing Photochemical Ozone Formation in the Pearl River Delta with a Photochemical Trajectory Model. *Atmos. Environ.* 44: 4199–4208.

Choi, Y.J. and Ehrman, S.H. (2004). Investigation of Sources of Volatile Organic carbon in the Baltimore Area Using Highly Time-resolved Measurements. *Atmos. Environ.* 38: 775–791.

Demir, S., Saral, A., Erturk, F., Kuzu, S.L., Goncaloglu, B.I. and Demir, G. (2012). Effect of Diurnal Changes in VOC Source Strengths on Performances of Receptor Models. *Environ. Sci. Pollut. Res.* 19: 1503–1514.

Draxler, R.R. and Hess, G. (1998). An Overview of the HYSPLIT_4 Modelling System for Trajectories. *Aust. Meteorol. Mag.* 47: 295–308.

Elbir, T., Banu, C., Eylem, C., Bayram, A. and Odabasi, M. (2007). Characterization of Volatile Organic Compounds (VOCs) and Their Sources in the Air of Izmir, Turkey. *Environ. Monit. Assess.* 133: 149–160.

Filella, I. and Penuelas, J. (2006). Daily, Weekly, and Seasonal Time Courses of VOC Concentrations in a Semi-urban Area near Barcelona. *Atmos. Environ.* 40: 7752–7769.

Gao, J., Wang, T., Ding, A. and Liu, C. (2005). Observational Study of Ozone and Carbon Monoxide at the Summit of Mount Tai (1534m asl) in Central-eastern China. *Atmos. Environ.* 39: 4779–4791.

Goldan, P.D., Kuster, W.C., Williams, E., Murphy, P.C., Fehsenfeld, F.C. and Meagher, J. (2004). Nonmethane Hydrocarbon and Oxy Hydrocarbon Measurements

during the 2002 New England Air Quality Study. *J. Geophys. Res.* 109: 1–14.

Guenther, A., Karl, T., Harley, P., Wiedinmyer, C., Palmer, P. and Geron, C. (2006). Estimates of Global Terrestrial Isoprene Emissions Using MEGAN (Model of Emissions of Gases and Aerosols from Nature). *Atmos. Chem. Phys. Discuss.* 6: 107–173.

Guo, H., Wang, T. and Louie, P. (2004). Source Apportionment of Ambient Non-methane Hydrocarbons in Hong Kong: Application of a Principal Component Analysis/Absolute Principal Component Scores (PCA/APCS) Receptor Model. *Environ. Pollut.* 129: 489–498.

Handl, G. (1997). Compliance Control Mechanisms and International Environmental Obligations. *Tul. J. Int'l & Comp. L.* 5: 29.

Hanson, D.J. (1996). Toxics Release Inventory Report Shows Chemical Emissions Continuing to Fall. *Chem. Eng.* 15: 29–30.

Kim, K.H., Shon, Z.H., Nguyen, H.T. and Jeon, E.C. (2011). A Review of Major Chlorofl Uorocarbons and their Halocarbon Alternatives in the Air. *Atmos. Environ.* 45: 1369–1382.

Kleindienst, T.E., Smith, D.F., Li, W., Edney, E.O., Driscoll, D.J., Speer, R.E. and Weathers, W.S. (1999). Secondary Organic Aerosol Formation from the Oxidation of Aromatic Hydrocarbons in the Presence of Dry Submicron Ammonium Sulfate Aerosol. *Atmos. Environ.* 3669–3681.

Kwok, E.S.C., Aschmann, S.M., Atkinson, R. and Arey, J. (1997). Products of the Gas-phase Reactions of o-, m- and p-xylene with the OH Radical in the Presence and Absence of NO_x. *J. Chem. Soc., Faraday Trans.* 93: 2847–2854.

Lai, C.H., Chen, K.S., Ho, Y.T., Peng, Y.P. and Chou, Y.M. (2005). Receptor Modeling of Source Contributions to Atmospheric Hydrocarbons in Urban Kaohsiung, Taiwan. *Atmos. Environ.* 39: 4543–4559.

Lanz, V.A., Buchmann, B., Hueglin, C., Locher, R., Reimann, S. and Staehelin, J. (2008). Factor analytical Modeling of C_2-C_7 Hydrocarbon Sources at an Urban Background Site in Zurich (Switzerland): Changes between 1993-1994 and 2005-2006. *Atmos. Chem. Phys. Discuss.* 8: 907–955.

Lee, B.S., Chiou, C.B. and Lin, C.Y. (2014). Analysis of Diurnal Variability of Atmospheric Halocarbons and CFC Replacements to Imply Emission Strength and Sources at an Urban Site of Lukang in Central Taiwan. *Atmos. Environ.* 99: 112–123.

Lee, S., Chiu, M., Ho, K., Zou, S. and Wang, X. (2002). Volatile Organic Compounds (VOCs) in Urban Atmosphere of Hong Kong. *Chemosphere* 48: 375–382.

Ling, Z.H., Guo, H., Cheng, H.R. and Yu, Y.F. (2011). Sources of Ambient Volatile Organic Compounds and their Contributions to Photochemical Ozone Formation at a Site in the Pearl River Delta, Southern China. *Environ. Pollut.* 159: 2310–2319.

Liu, H.W., Wu, B.Z., Nian, H.C., Chen, H.J., Lo, J.G. and Chiu, K.H. (2012). VOC Amounts in Ambient Areas of a High-technology Science Park in Taiwan: their Reciprocal

Correlations and Impact on Inhabitants. *Environ. Sci. Pollut. Res.* 19: 303–312.

Liu, Y., Shao, M., Lu, S.H., Chang, C.C., Wang, J.L. and Fu, L. (2008a). Source Apportionment of Ambient Volatile Organic Compounds in the Pearl River Delta, China: Part II. *Atmos. Environ.* 42: 6261–6274.

Liu, Y., Shao, M., Lu, S.H., Chang, C.C., Wang, J.L. and Gao, C. (2008b). Volatile Organic Compound (VOC) Measurements in the Pearl River Delta (PRD) Region, China. *Atmos. Chem. Phys.* 8: 1531–1545.

Lonneman, W.A., Seila, R.L. and Meeks, S.A. (1986). Non-methane Organic Composition in the Lincoln Tunnel. *Environ. Sci. Technol.* 20: 790–796.

Lyu, Y.B., Tan, L., Teng, E.J., Wang, C., Lyu, T.F. and Liang, X. (2013). Concentration Levels and Composition Characteristics of VOCs at the Background Locations in China. *Environ. Chem.* 0254: 726–733.

Mao, T., Wang, Y.S., Jiang, J., Wu, F.K. and Wang, M. (2008). The Vertical Distributions of VOCs in the Atmosphere of Beijing in Autumn. *Sci. Total Environ.* 390: 97–108.

Mao, T., Wang, Y.S., Xu, H.H., Jiang, J., Wu, F.K. and Xu, X.B. (2009). A Study of the Atmospheric VOCs of Mount Tai in June 2006. *Atmos. Environ.* 43: 2503–2508.

Martinerie, P., Nourtier-Mazauric, E., Barnola, J.M., Sturges, W.T., Worton, D.R., Atlas, E., Gohar, L.K., Shine, K.P. and Brasseur, G.P. (2009). Long-lived Halocarbon Trends and Budgets from Atmospheric Chemistry Modelling Constrained with Measurements in Polar Firn. *Atmos. Chem. Phys.* 9: 3911–3934.

Molina, M.J. and Rowland, F.S. (1974). Stratospheric Sink for Chlorofluoromethanes: Chlorine Atom-catalysed Destruction of Ozone. *Nature* 249: 810–812.

Monod, A., Sive, B.C., Avino, P., Chen, T., Blake, D.R. and Sherwood Rowland, F. (2001). Monoaromatic Compounds in Ambient Air of Various Cities: A Focus on Correlations between the Xylenes and Ethylbenzene. *Atmos. Environ.* 35: 135–149.

Montzka, S.A., Butler, J.H., Myers, R.C., Thompson, T.M., Swanson, T.H., Clarke, A.D., Lock, L.T. and Elkins, J.W. (1996). Decline in the Tropospheric Abundance of Halogen from Halocarbons: Implications for Stratospheric Ozone Depletion. *Science* 272: 1318–1322.

Moreira dos Santos, C.Y., de Almeida Azevedo, D. and de Aquino Neto, F.R. (2004). Atmospheric Distribution of Organic Compounds from Urban Areas near a Coal-Fired Power Station. *Atmos. Environ.* 38: 1247–1257.

Oguz, O., Karman, D. and Tuncel, G. (2003). Measurement of Traffic Related Toxic Air Pollutants in an Urban Atmosphere. *Water Air Soil Pollut.* 3: 255–267

Pugh, T.A.M., Ashworth, K., Wild, O. and Hewitt, C.N. (2013). Effects of the Spatial Resolution of Climate Data on Estimates of Biogenic Isoprene Emissions. *Atmos. Environ.* 70: 1–6.

Seinfeld, J.H. and Pandis, S.N. (2006). *Atmospheric Chemistry and Physics: from Air Pollution to Climate Change*, Wiley, New York.

Sentian, J., Xiang, C.T., Jing, H.C., Quack, B., Fuhlbrügge, S., Krüger, K. and Atlas, E. (2015). Observation of the Variations of Very Short-Lived Halocarbon Emissions in Tropical Coastal Marine Boundary Layer. *Adv. Sci. Lett.* 21: 144–149.

Simpson, W., von Glasow, R., Riedel, K., Anderson, P., Ariya, P., Bottenheim, J., Burrows, J., Carpenter, L., Frieß, U. and Goodsite, M.E. (2007). Halogens and their Role in Polar Boundary-layer Ozone Depletion. *Atmos. Chem. Phys.* 7: 4375–4418.

Sindelarova, K., Granier, C., Bouarar, I., Guenther, A., Tilmes, S., Stavrakou, T., Müller, J.F., Kuhn, U., Stefani, P. and Knorr, W. (2014). Global Data Set of Biogenic VOC Emissions Calculated by the MEGAN Model over the Last 30 Years. *Atmos. Chem. Phys.* 14: 9317–9341.

Sun, M., Wang, Y., Wang, T., Fan, S., Wang, W., Li, P., Guo, J. and Li, Y. (2010). Cloud and the Corresponding Precipitation Chemistry in South China: Water-soluble Components and Pollution Transport. *J. Geophys. Res.* 115: D22303, doi: 10.1029/2010JD014315.

Suthawaree, J., Tajima, Y., Khunchornyakong, A., Kato, S., Sharp, A. and Kajii, Y. (2012). Identification of Volatile Organic Compounds in Suburban Bangkok, Thailand and their Potential for Ozone Formation. *Atmos. Res.* 104–105: 245–254.

Tang, J.H., Chan, L.Y., Chan, C.Y., Li, Y.S., Chang, C.C., Liu, S.C., Wu, D. and Li, Y.D. (2007). Characteristics and Diurnal Variations of NMHCs at Urban, Suburban, and Rural Sites in the Pearl River Delta and a Remote Site in South China. *Atmos. Environ.* 8620–8632.

Tang, J., Chan, L., Chan, C., Li, Y., Chang, C., Wang, X., Zou, S., Barletta, B., Blake, D. and Wu, D. (2008). Implications of Changing Urban and Rural Emissions on Non-methane Hydrocarbons in the Pearl River Delta Region of China. *Atmos. Environ.* 42: 3780–3794.

Tang, X., Yuanhang, Z. and Min, S. (2006). A*tmospheric Environment Chemitry*. Higher Education Press.

Tang, X.Y., Zhang, Y.H. and Shao, M. (2006). *Atmospheric Environmental Chemistry*, Higher Education Press.

Volkamer, R., Jimenez, J.L., San Martini, F., Dzepina, K., Zhang, Q., Salcedo, D., Molina, L.T., Worsnop, D.R. and Molina, M.J. (2006). Secondary Organic Aerosol Formation from Anthropogenic Air Pollution: Rapid and Higher than Expected. *Geophys. Res. Lett.* 33: L17811, doi: 10.1029/2006GL026899.

Wagner, P. and Kuttler, W. (2014). Biogenic and Anthropogenic Isoprene in the Near-surface Urban Atmosphere — A Case Study in Essen, Germany. *Sci. Total Environ.* 475: 104–115.

Wang, C., Shao, M., Huang, D., Lu, S., Zeng, L., Hu, M. and Zhang, Q. (2014). Estimating Halocarbon Emissions Using Measured Ratio Relative to Tracers in China. *Atmos. Environ.* 89: 816–826.

Wang, H., Lou, S., Huang, C., Qiao, L., Tang, X., Chen, C., Zeng, L., Wang, Q., Zhou, M., Lu, S. and Yu, X. (2014). Source Profiles of Volatile Organic Compounds from Biomass Burning in Yangtze River Delta, China. *Aerosol Air Qual. Res.* 14: 818–828.

Wang, Y., Ren, X., Ji, D., Zhang, J., Sun, J. and Wu, F. (2012). Characterization of Volatile Organic Compounds in the Urban Area of Beijing from 2000 to 2007. *J.*

Environ. Sci. 24: 95–101.

Watson, J.G., Chow, J.C. and Fujita, E.M. (2001). Review of Volatile Organic Compound Source Apportionment by Chemical Mass Balance. *Atmos. Environ.* 35: 1567–1584.

Wu, F.K., Wang, Y.S., An, J.L. and Zhang, J.G. (2010). Study on Concentration, Ozone Production Potential and Sources of VOCs in the Atmosphere of Beijing during Olympic Period. *Chin. J. Environ. Sci.* 31 10–16.

Yurdakul, S., Civan, M. and Tuncel, G. (2013). Volatile Organic Compounds in Suburban Ankara Atmosphere, Turkey: Sources and Variability. *Atmos. Res.* 120: 298–311.

Zhang, J., Sun, Y., Wu, F., Sun, J. and Wang, Y. (2014). The Characteristics, Seasonal Variation and Source Apportionment of VOCs at Gongga Mountain, China. *Atmos. Environ.* 88: 297–305.

Zheng, J., Shao, M., Che, W., Zhang, L., Zhong, L., Zhang, Y. and Streets, D. (2009). Speciated VOC Emission Inventory and Spatial Patterns of Ozone Formation Potential in the Pearl River Delta, China. *Environ. Sci. Technol.* 43: 8580–8586.